arXiv:1109.3962v2 [cond-mat.supr-con] 9 Dec 2011

Fe-doping induced superconductivity in charge-density-wave system 1T-TaS$_2$

L. J. Li,[1] W. J. Lu,[1,*] X. D. Zhu,[2] L. S. Ling,[2] Z. Qu,[2] and Y. P. Sun[1,2,†]
[1]*Key Laboratory of Materials Physics, Institute of Solid State Physics,*
Chinese Academy of Sciences, Hefei 230031, People's Republic of China
[2]*High Magnetic Field Laboratory, Chinese Academy of Sciences, Hefei 230031, People's Republic of China*

(Dated: December 12, 2011)

We report the interplay between charge-density-wave (CDW) and superconductivity of 1T-Fe$_x$Ta$_{1-x}$S$_2$ ($0 \leq x \leq 0.05$) single crystals. The CDW order is gradually suppressed by Fe-doping, accompanied by the disappearance of pseudogap/Mott-gap as shown by the density functional theory (DFT) calculations. The superconducting state develops at low temperatures within the CDW state for the samples with the moderate doping levels. The superconductivity strongly depends on x within a narrow range, and the maximum superconducting transition temperature is 2.8 K as $x = 0.02$. We propose that the induced superconductivity and CDW phases are separated in real space. For high doping level ($x > 0.04$), the Anderson localization (AL) state appears, resulting in a large increase of resistivity. We present a complete electronic phase diagram of 1T-Fe$_x$Ta$_{1-x}$S$_2$ system that shows a dome-like $T_c(x)$.

PACS numbers: 74.70.-b, 71.45.Lr, 71.10.Hf, 74.25.Jb

I. INTRODUCTION

The relationship between superconductivity and charge-density-wave (CDW) is debated for several decades. The idea that superconductivity and CDW are competing electronic states is one of the fundamental concepts of condensed-matter physics,[1–3] and the coexistence of superconductivity and other electronic states is the other one.[4–6] For high-T_c copper oxide superconductor, the magnetic order and superconductivity nearly has no overlapping from the phase diagram, while for Fe-based superconductor the coexistence of spin-density-wave (SDW) and superconductivity can be clearly observed.[1–4,7] And for transition-metal dichalcogenide compounds (TMDCs) MX$_2$ where M is a group 4 or 5 metal and X=S, Se, or Te, the experimental results have shown that the charge-order can boost superconductivity in an electron-phonon coupled system 2H-NbSe$_2$,[8] and the CDW and superconductivity states can coexist in 1T-Cu$_x$TiSe$_2$,[9–11] while there is a competition between the superconductivity and the CDW in 2H-Na$_x$TaS$_2$ system.[12] So the nature of the interplay between CDW and superconductivity remains to be further elucidated, and the layered TMDCs may be one of the ideal candidates.

In the family of TMDCs, two basic structures of TaS$_2$ were found and defined by the different orientation of stacking chalcogensheets, one is 2H-TaS$_2$ with Ta in trigonal prismatic coordination with S atoms, and the other one is 1T-TaS$_2$ with Ta in octahedral coordination with S atoms. For 1T-TaS$_2$, with decreasing temperature, exhibits incommensurate, nearly commensurate, and commensurate CDWs.[13,14] The commensurate CDW (CCDW) phase accompanies periodic lattice distortions that form a supercell with star-of-David clusters.[15] The CDW can induce the gap near the Fermi level by the lattice distortions. However, the CDW insulating phase can be inhibited by the external pressure,[14] disorder,[16] and photo-excitation[17] in 1T-TaS$_2$ system, and hence the metallic state or superconductivity may arise in this system. It is worthwhile to investigate 1T-TaS$_2$ system by doping, since the doping can effectively modify the band structure by altering the crystal structure and carriers concentration, and thereby affect the CDW state and potentially induce new collective states.

In this paper, we present the combined experimental and theoretical studies of the superconductivity of 1T-Fe$_x$Ta$_{1-x}$S$_2$ single crystals and report a complete electronic phase diagram of 1T-Fe$_x$Ta$_{1-x}$S$_2$ system which shows a dome-like $T_c(x)$. This finding complements the recent discovery of pressure induced superconductivity in 1T-TaS$_2$.[14]

II. EXPERIMENT

The 1T-Fe$_x$Ta$_{1-x}$S$_2$ single crystals were grown via the chemical vapor transport (CVT) method with iodine as a transport agent, the sample stoichiometry and structure were verified by X-ray energy dispersive spectroscopy (EDS) of a scanning electron microscope (SEM) and inductively coupled plasma atomic emission spectrometry (ICP-AES). The resistivity and the Seebeck effect were measured in a Quantum Design physical property measurement system (PPMS), and the magnetization measurements were performed on a superconducting quantum interference device (SQUID) system. The electronic structure calculations were performed in the framework of density functional theory (DFT) within the local-density approximation (LDA), using the ABINIT code.[18] Normconserving pseudopotentials and a plane-wave basis set with a kinetic energy cutoff of 1600 eV were used. For the undistorted 1T-phase a $14 \times 14 \times 8$ Monkhorst k-point sampling was used, while for the CCDW phase, a $6 \times 6 \times 8$ mesh of k-point was used. In order to describe the strong correlation of electrons in Mott-Hubbard physics,

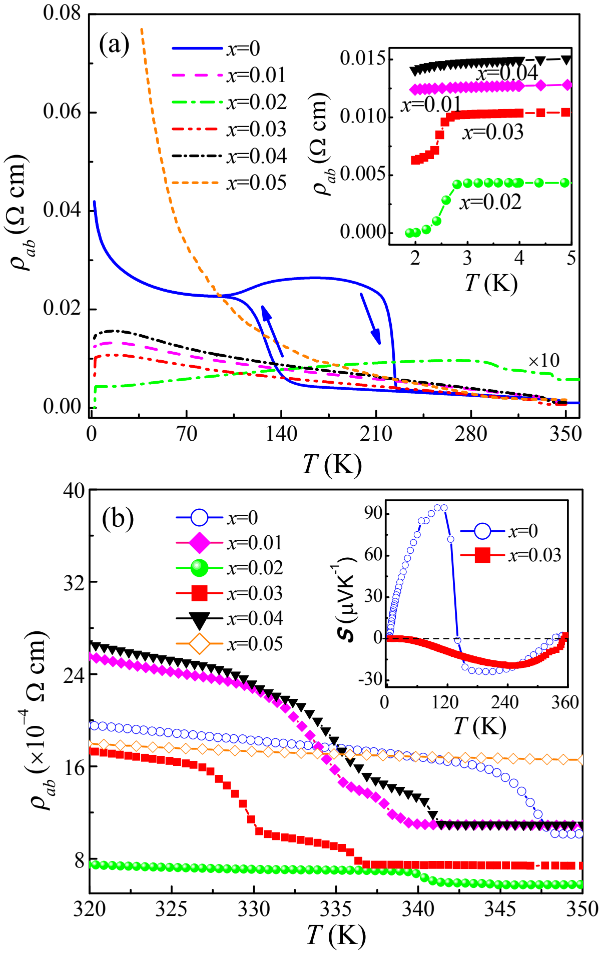

FIG. 1. (a) Temperature dependent in-plane resistivity $\rho_{ab}(T)$ of $1T$-$Fe_xTa_{1-x}S_2$ single crystals. Inset shows the detail of superconducting transitions. (b) The NCCDW transitions near 350K of all the samples. Inset shows the temperature dependence of the thermopower of $1T$-$Fe_xTa_{1-x}S_2$ crystals for $x = 0$ and 0.03.

we adopted a LDA+U method where U is the onsite Coulomb repulsion.

III. RESULTS AND DISCUSSION

The in-plane resistivity (ρ_{ab}) measurements on $1T$-$Fe_xTa_{1-x}S_2$ single crystals using standard 4-point technique are shown in Fig. 1(a). For the $x \leq 0.04$ samples, the resistivity decreases with the increasing of x until $x > 0.02$ and then increases. For the $x > 0.04$ samples, the resistivity shows large increase especially in the low-temperatures range, which should be due to the Anderson localization (AL) of the conduction electrons by the random potential, which is consistent with the early reports.[19,20] Furthermore, the low-temperature CCDW phase is suppressed for $x \geq 0.01$, and interestingly the signature of superconductivity appears at 2.8 and 2.6 K for $x = 0.02$ and 0.03, respectively, while no superconductivity appears for $x \geq 0.04$ down to 2 K (see the inset of Fig. 1(a)). The maximum zero resistivity temperature is about 2.1 K at $x = 0.02$. So it may be the optimal doping and we study this composition in detail in the following part.

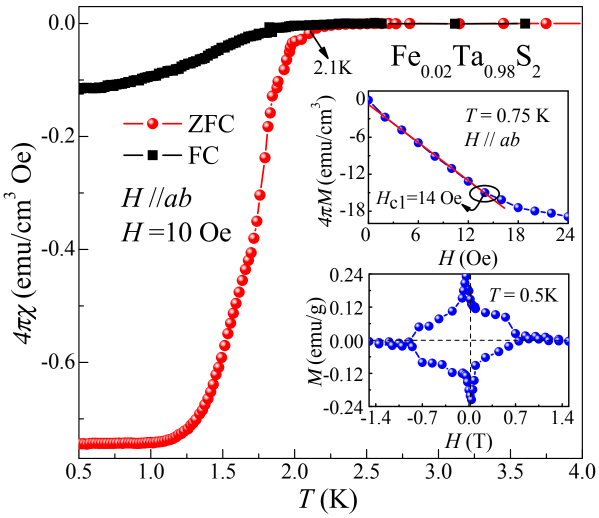

FIG. 2. Temperature dependence of magnetic susceptibility of $1T$-$Fe_{0.02}Ta_{0.98}S_2$ single crystals. The right top inset shows the initial $4\pi M(H)$ isotherm at 0.75 K, and the red line shows the linear fitting in the low field range. The right bottom inset shows the magnetization hysteresis loops of $1T$-$Fe_{0.02}Ta_{0.98}S_2$ at $T = 0.5$ K as $H \parallel ab$.

The transitions from the incommensurate CDW (ICCDW) to the nearly CCDW (NCCDW) at high temperatures, which behave as the resistivity suddenly increases in the temperature range of 350-330 K, keep existing as $x \leq 0.04$ (see Fig. 1(b)). The inset of Fig. 1(b) shows the temperature dependence of thermopower (S) for the $x = 0$ and 0.03 samples. For the $x = 0$ sample, S changes signs at about 350 K and 140 K, which can be attributed to the NCCDW and CCDW transitions, respectively.[21] While there is only one transition at about 340 K for the $x = 0.03$ sample. This observation is in agreement with the step in the resistivity curve that is corresponding to the NCCDW phase transition. It indicates that the CCDW phase disappears, while the NCCDW phase still remains even after 3% Fe doping. Moreover, the Seebeck coefficient of the $x = 0.03$ sample becomes more negative in the whole temperature range, suggesting that Fe acts at least in part as an n-type doping.

The temperature dependence of magnetic susceptibility for $Fe_{0.02}Ta_{0.98}S_2$ at 10 Oe as $H \parallel ab$ is plotted in Fig. 2. The diamagnetism appears in the low temperature region, which further confirms the existence of superconductivity. Also the steep transition in $M(T)$ curve indicates that the sample is rather homogeneous. The superconducting transition temperature is about 2.1 K

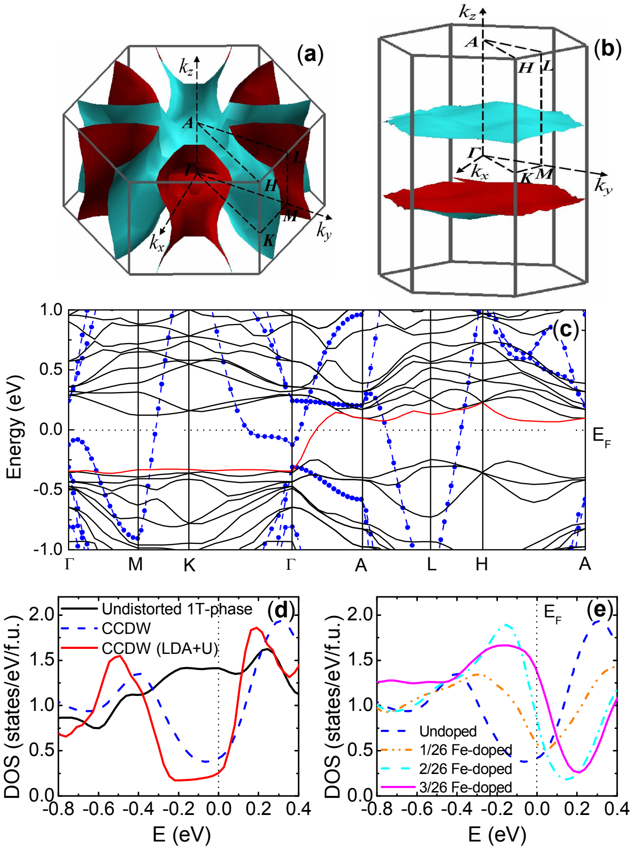

FIG. 3. (a) Fermi surface for the undistorted $1T$ structure and (b) reconstructed CCDW superstructure. (c) Energy band structure near the Fermi level for the undistorted $1T$-phase (blue points) and the reconstructed CCDW superstructure (solid lines). The band that crosses the Fermi level is plotted as a red line. (d) Density of states near the Fermi level for the un-doped $1T$-TaS$_2$ and (e) the Fe-doped system.

that is defined by the onset point of the zero-field-cooling (ZFC) and field-cooling (FC) curves . The smaller magnetization value for FC is likely due to the complicated magnetic flux pinning effects.[22] The value of -$4\pi\chi$ at 0.5 K is about 75% where the demagnetization factor is negligible for $H \parallel ab$, implying the bulk superconductivity of Fe$_{0.02}$Ta$_{0.98}$S$_2$ sample.

The right top inset of Fig. 2 shows the initial $M(H)$ curve of $1T$-Fe$_{0.02}$Ta$_{0.98}$S$_2$ in the low field region at 0.75 K as $H \parallel ab$, the solid line shows the linear fitting for the low field range. The obtained slope of the linear fitting up to 15 Oe of our measurement at 0.75 K is -0.98(6), and this corresponds to $-4\pi M = H$ as $H \parallel ab$, describing the Meissner shielding effects. And from the deviated point of the fitting line we can obtain the lower superconducting critical field $H_{c1}(0.75K) = 14$ Oe. The right bottom inset of Fig. 2 shows the magnetization hysteresis loop of $1T$-Fe$_{0.02}$Ta$_{0.98}$S$_2$ at 0.5 K as $H \parallel ab$, and the shape of the $M(H)$ curves shows that $1T$-Fe$_{0.02}$Ta$_{0.98}$S$_2$ is a typical type-II superconductor.

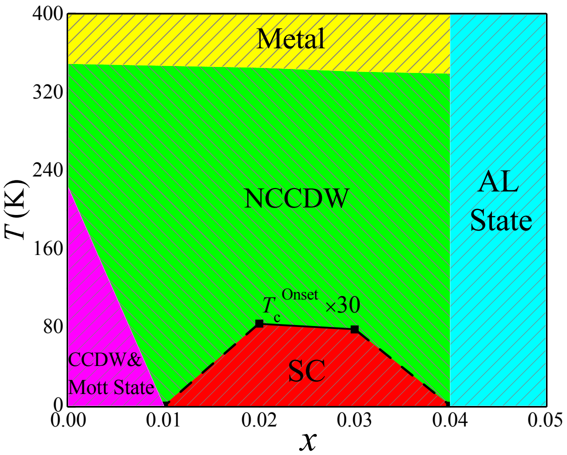

FIG. 4. The electronic phase diagram of $1T$-Fe$_x$Ta$_{1-x}$S$_2$ single crystals.

In order to elucidate the Fe-doping effect on the properties of the host $1T$-TaS$_2$, we carried out theoretical calculation by DFT (shown in Fig. 3). We model the $\sqrt{13} \times \sqrt{13} \times 2$ supercell which contains at least one-site substitution of Ta atom by Fe atom (1/26 doping level). Figures 3(a) and 3(b) show the calculated Fermi surfaces (FS) for the undistorted $1T$ structure and the reconstructed CCDW superstructure, respectively, which clearly show that the undistorted $1T$-TaS$_2$ has a quasi-two-dimensional Fermi surface, while the CCDW phase has a quasi-one-dimensional Fermi surface. Figure 3(c) shows the calculated energy band structure near the Fermi leve for the ideal/undistorted $1T$-phase and the reconstructed CCDW superstructure. For the ideal/undistorted $1T$ structure, the Ta-d bands cross the Fermi level E_F and strongly disperse along Γ-M-K-Γ and A-L-H-A, which leads to a good metallic character. Along Γ-A only weak dispersion on the Fermi level is left, consistent with the quasi-2D character of the $1T$-phase structure. The relaxed CCDW structure shows the star-of-David clusters in which the first and second rings of Ta atoms averagely contract inwards by 5-6%. The Ta star-of-David clusters lead the Ta-d state to become localized in the in-plane directions, which results in a localized uppermost band along Γ-M-K-Γ at about -0.3 eV. The band at the Fermi level disperses only along Γ-A direction, indicating the existence of quasi-one-dimensional Fermi surface (see Fig. 3(b)) that allows that electrons conduct only along the c-axis, and the ab-plane conductivity becomes worse in CCDW structure.

Figure 3(d) shows the density of states (DOS) for the undistorted $1T$-TaS$_2$ and the distorted CCDW structure. For the undistorted $1T$-phase, a large DOS locates at the Fermi level. However, in the CCDW structure, the DOS near the Fermi level shows a pseudogap structure, resulting in a semimetal conduction. Considering the correlation of Ta-d electrons, we applied LDA+U method to the

CCDW structure, where the effective on-site Coulomb U is set to be 0.5 eV (by using this value, the calculated gap is closed to the experimentally observed gap of 180 meV from angle-resolved photoemission spectroscopy[23]). The calculated results show that a deep Mott gap develops and the localized states form at the Fermi level, which accounts for the experimentally observed insulating conduction behavior at low temperatures. By Fe-doping, the energy gap disappears due to the suppression of CCDW distortions (see Fig. 3(e)), and also the Fe-3d band partially contributes to the DOS at the Fermi level (the calculated atom-projected DOS are not shown in figures), which could contribute to the metallic character for $\mathrm{Fe}_x\mathrm{Ta}_{1-x}\mathrm{S}_2$ and consistent with the thermopower results.

Finally, the overall behavior of this system is summarized as the electronic phase diagram presented in Fig. 4. By using Fe doping as a controlled tuning parameter, the CDW transition of 1T-TaS_2 is driven in temperature, and a new superconducting state emerges. The dependence of the superconducting transition temperature on the iron content $T_c(x)$ shows a domelike structure, characteristically found in the electronic phase diagrams of some heavy fermion and layered organic superconductors.[24–26] Furthermore, the superconductivity strongly depends on x, and only occurs in the narrow doping level. The superconductivity appears for $x > 0.01$, going through a maximum of 2.8 K as $x = 0.02$, followed by a decrease before the chemical phase boundary ($x = 0.04$) is reached. The Fe-doping results in a tendency towards breaking the long-range CCDW order. The superconductivity can develop within the metallic interdomain regions in the NCCDW phase. The induced superconductivity and the CDW compete with each other and are of intrinsic phase-separation character. On the other hand the electron-phonon interaction in CDW domains may also play an important role in the observed superconductivity.[27] The similar superconductivity induced by K-doping upon inhibiting the long-range CDW order in BaBiO_3 system was observed previously.[28] As $x \geq 0.05$, the Anderson localization state due to the random potential results in a large resistivity increase, especially for low temperature resistivity.

IV. CONCLUSION

In summary, we have investigated the 1T-$\mathrm{Fe}_x\mathrm{Ta}_{1-x}\mathrm{S}_2$ single crystals by experiment and theoretical calculation and presented the electronic phase diagram for 1T-$\mathrm{Fe}_x\mathrm{Ta}_{1-x}\mathrm{S}_2$ single crystals. We found that with the suppression of the CCDW, the superconducting state appears at low temperatures as $0.01 < x < 0.04$, while the NCCDW exists all the same. It may suggest that these two phases can coexist and keep the balance in favor of superconductivity until $x \geq 0.04$. We propose that the induced superconductivity and CDW phases are separated in real space. The maximum superconducting transition temperature is 2.8 K as $x = 0.02$, and a dome-like $T_c(x)$ is obtained. The calculated DOS near the Fermi level for the un-doped and the Fe-doped 1T-TaS_2 show that the Mott gap disappears after Fe doping and the Fe-3d band partially contributes to the DOS at the Fermi level, which may contribute to the metallic and superconducting character. For $x > 0.04$, the Anderson localization state appears, resulting in a large increase of resistivity.

ACKNOWLEDGMENTS

This work was supported by the National Key Basic Research under contract No. 2011CBA00111, and the National Nature Science Foundation of China under contract Nos. 10804111, 10974205, 11104279 and 51102240, and Director's Fund of Hefei Institutes of Physical Science, Chinese Academy of Sciences. The DFT calculations were partially performed at the Center for Computational Science of CASHIPS.

---

[*] Corresponding author. E-mail: wjlu@issp.ac.cn

[†] Corresponding author. E-mail: ypsun@issp.ac.cn

[1] H. Luetkens, H. -H. Klauss, M. Kraken, F. J. Litterst, T. Dellmann, R. Klingeler, C. Hess, R. Khasanov, A. Amato, C. Baines, M. Kosmala, O. J. Schumann, M. Braden, J. Hamann-Borrero, N. Leps, A. Kondrat, G. Behr, J. Werner, and B. Büchner, Nature Mater. **8**, 305 (2009).

[2] J. Zhao, Q. Huang, C. D. L. Cruz, S. L. Li, J. W. Lynn, Y. Chen, M. A. Green, G. F. Chen, G. Li, Z. Li, J. L. Luo, N. L. Wang, and P. C. Dai, Nature Mater. **7**, 953 (2008).

[3] H. Bakrim and C. Bourbonnais, Europhys. Lett. **90**, 27011 (2010).

[4] M. D. Lumsden, A. D. Christianson, E. A. Goremychkin, S. E. Nagler, H. A. Mook, M. B. Stone, D. L. Abernathy, T. Guidi, G. J. MacDougall, C. de la Cruz, A. S. Sefat, M. A. McGuire, B. C. Sales, and D. Mandrus, Nature Phys. **6**, 182 (2010).

[5] J. A. Wilson and A. D. Yoffe, Adv. Phys. **28**, 193 (1969).

[6] A. H. Castro Neto, Phys. Rev. Lett. **86**, 4382 (2001).

[7] H. Matsui, K. Terashima, T. Sato, T. Takahashi, M. Fujita, and K. Yamada, Phys. Rev. Lett. **95**, 017003 (2005).

[8] T. Kiss, T. Yokoya, A. Chainani, S. Shin, T. Hanaguri, M. Nohara, and H. Takagi, Nature Phys. **3**, 720 (2007).

[9] E. Morosan, H. W. Zandbergen, B. S. Dennis, J. W. G. Bos, Y. Onose, T. Klimczuk, A. P. Ramirez, N. P. Ong, and R. J. Cava, Nature Phys. **2**, 544(2006).

[10] D. Qian, D. Hsieh, L. Wray, E. Morosan, N. L. Wang, Y. Xia, R. J. Cava, and M. Z. Hasan, Phys. Rev. Lett. **98**, 117007 (2007).

[11] J. F. Zhao, H. W. Ou, G. Wu, B. P. Xie, Y. Zhang, D. W. Shen, J. Wei, L. X. Yang, J. K. Dong, M. Arita, H. Namatame, M. Taniguchi, X. H. Chen, and D. L. Feng, Phys. Rev. Lett. **99**, 146401 (2007).

[12] L. Fang, Y. Wang, P. Y. Zou, L. Tang, Z. Xu, H. Chen, C. Dong, L. Shan, and H. H. Wen, Phys. Rev. B **72**, 014534 (2005).

[13] J. A. Wilson, F. J. Di Salvo, and S. Mahajan, Adv. Phys. **24**, 117 (1975).

[14] B. Sipos, A. F. Kusmartseva, A. Akrap, H. Berger, L. Forró, and E. Tutiš, Nature Mater. **7**, 960 (2008).

[15] F. Clerc, C. Battaglia, H. Cercellier, C. Monney, H. Berger, L. Despont, M. G. Garnier, and P. Aebi, J. Phys.: Condens. Matter **19**, 355002 (2007).

[16] P. Xu, J. O. Piatek, P. -H. Lin, B. Sipos, H. Berger, L. Forró, H. M. Rønnow, and M. Grioni, Phy. Rev. B **81**, 172503 (2010).

[17] N. Dean, J. C. Petersen, D. Fausti, R. I. Tobey, S. Kaiser, L. V. Gasparov, H. Berger, and A. Cavalleri, Phys. Rev. Lett. **106**, 016401 (2011).

[18] X. Gonze, J. -M. Beuken, R. Caracas, F. Detraux, M. Fuchs, G. -M. Rignanese, L. Sindic, M. Verstraete, G. Zerah, F. Jollet, M. Torrent, A. Roy, M. Mikami, Ph. Ghosez, J. -Y. Raty, and D. C. Allan, Comput. Mater. Sci. **25**, 478 (2002).

[19] F. J. Di Salvo, J. A. Wilson, and J. V. Waszczak, Phys. Rev. Lett. **36**, 885 (1976).

[20] R. M. Fleming and R. V. Coleman, Phys. Rev. Lett. **34**, 1502 (1975).

[21] T. Tani and S. Tanaka, J. Phys. Soc. Jpn. **53**, 1790 (1984).

[22] D. E. Prober, M. R. Beasley, and R. E. Schwall, Phys. Rev. B **15**, 5245 (1977).

[23] Th. Pillo, J. Hayoz, D. Naumović, H. Berger, L. Perfetti, L. Gavioli, A. Taleb-Ibrahimi, L. Schlapbach, and P. Aebi, Phys. Rev. B **64**, 245105 (2001).

[24] P. A. Lee, N. Nagaosa, and X. -G. Wen, Rev. Mod. Phys. **78**, 17 (2006).

[25] V. A. Sidorov, M. Nicklas, P. G. Pagliuso, J. L. Sarrao, Y. Bang, A. V. Balatsky, and J. D. Thompson, Phys. Rev. Lett. **89**, 157004 (2002).

[26] J. Wosnitza, J. Low Temp. Phys. **146**, 641 (2007).

[27] A. Y. Liu, Phys. Rev. B **79**, 220515 (2009).

[28] K. Iwano and K. Nasu, Phys. Rev. B **57**, 6957 (1998).